Journal of Molecular Structure 1344 (2025) 142963

Contents lists available at ScienceDirect

Journal of Molecular Structure

journal homepage: www.elsevier.com/locate/molstr

Aldose reductase inhibitory activity, molecular docking,ADMET, and density functional theory investigation of flavonoids isolated from *Euphorbia pulcherrima* Willd Ex Koltz

Rahaf Ajaj [a,*], Abdur Rauf [b,*], Zuneera Akram [c], Muhammad Umer Khan [d], Raima Rehman [e], Zubair Ahmad [b], Yasir Anwar [f], Marcello Iriti [g,h,*]

[a] Department of Environmental and Public Health, College of Health Sciences, Abu Dhabi University, Abu Dhabi, United Arab Emirates
[b] Department of Chemistry, University of Swabi, Swabi, Anbar, 23561, Khyber Pakhtunkhwa (K.P.), Pakistan
[c] Department of Pharmacology, Faculty of Pharmaceutical Sciences, Baqai Medical University, Karachi, Pakistan
[d] Institute of Molecular Biology and Biotechnology, The University of Lahore, Lahore, Pakistan
[e] Centre of Excellence in Molecular Biology, University of the Punjab, Lahore Pakistan
[f] Department of Biological Sciences, Faculty of Science, King Abdulaziz University, Jeddah, Saudi Arabia
[g] Department of Biomedical, Surgical and Dental Sciences, University of Milan, via Luigi Vanvitelli 32, 20129, Milan, Italy
[h] National Interuniversity Consortium of Materials Science and Technology (INSTM), 50121 Firenze, Italy

ARTICLE INFO

Keywords:
E. pulcherrima
Flavonoids
Diabetes mellitus
Hyperglycemia
Aldose reductase

ABSTRACT

Diabetes mellitus is a chronic metabolic disease associated with severe complications includingdiabetes cataracts which results from accumulating sorbitol in tissues due to aldose reductaeoveractivity. Approaches that would selectively modulate AR to prevent sorbitol accumulation have become one of the basic strategies for managing diabetes-linked complications.This study examines the two flavonoids derived from *E. pulcherrima*, 5,7,8,3′,4′-pentahydroxy-3- methoxyflavone (**1**), and kaempferol-3-β-D glucopyranosyl (**2**), and their potential to suppress AR activity. Compounds exhibited potent inhibitory effects with IC_{50} values of 0.97 ± 0.53 μM and 0.92 ± 0.48 μM, respectively. These results are close to the SC-13,153 standard inhibitor, d-saccharic acid 1,4-lactone, with an IC_{50} equal to 0.88 ± 0.34 μM. *In silico* molecular docking examined these flavonoids' interaction with AR more strongly (compound **2**: -10.248 kcal/mol and compound **1**: -9.629 kcal/mol) and showed that such complexation was stable at the enzyme's active site. The interaction analysisindicated that compound **1**and compound **2** specifically bind through polar hydrogen bonding and hydrophobic interactions. In addition to docking, DFT calculations revealed compound 1 had a lower energy gap (3.02 eV) compared to compound 2 (3.84 eV), suggesting higher reactivity and stability for enzyme inhibition. The molecular electrostatic potential (MESP) surface mapping indicated well-distributed charge regions, favoring electrophilic and nucleophilic interactions.The molecular dynamics (MD) simulations investigation revealed the RMSD value (<2.5Å), suitable fluctuation in RMSF, and compactness of protein in ROG analysis for compound 1. Moreover, the MMGBSA analysis showedhigher binding free energy for compound 1 (-38.458 kcal/mol), highlighting the potential inhibitory efficiency of the compound.Therefore, *E. pulcherrima* flavonoids can be an effective natural AR inhibitor with a therapeutic application for treating hyperglycemia-connected complications. These compounds might be even more effective and less toxic than synthetic AR inhibitors, opening a new way for plant-based diabetes treatment.

1. Introduction

Diabetes mellitus is a chronic and progressively disabling disease that gradually affects a large part of the world population despite advances in treatment and prevention strategies, and this disease represents a global health problem due to its dangerous complications.

* Corresponding authors.
E-mail addresses: rahaf.ajaj@adu.ac.ae (R. Ajaj), mashaljcs@yahoo.com (A. Rauf), dr.zunaira@baqai.edu.pk (Z. Akram), muhammad.umer4@mlt.uol.edu.pk (M.U. Khan), raima.rehman01@gmail.com (R. Rehman), za3724364@gmail.com (Z. Ahmad), yanwarulhaq@kau.edu.sa (Y. Anwar), marcello.iriti@unimi.it (M. Iriti).

https://doi.org/10.1016/j.molstruc.2025.142963
Received 15 April 2025; Received in revised form 3 June 2025; Accepted 9 June 2025
Available online 9 June 2025

Memon and Khalid (2002) have postulated that among various complications associated with diabetes, microvascular complications, including diabetic cataracts, bear the most significant disease burden [1]. This condition mainly occurs due to hyperglycemia, which triggers several biochemical paths, especially the polyol pathway. Ahmad et al. (2024) [2] noted that under hyperglycemia tissues, glucose is converted to sorbitol through the enzyme aldose reductase (AR); this leads to osmotic or oxidative stress in lens cells, a crucial pathway in cataract development. This knowledge of the road map of AR and the methods used to halt the execution of this process has become the foundation of therapeutic regimens to prevent diabetes-induced complications, keep patient survival rates high and decrease the cases of diabetic cataracts.

A polyol pathway enzyme, aldose reductase, is a rate-limiting enzyme that utilizes nicotinamide adenine dinucleotide phosphate (NADPH) to convert glucose to sorbitol [3]. Singh et al. (2021) pointed out that under normoglycemic conditions, aldose reductase exhibits low enzymatic activity, playing a limited role in overall glucose metabolism [4]. Nonetheless, worsening hyperglycemic conditions and hyperactivity of this pathway will lead to the intracellular accumulation of sorbitol, which results in osmotic stress, cell swelling and oxidative stress. These effects are more detrimental to non-insulin dependent tissue such as lens, retina, kidney and peripheral nerves where sorbitol accumulation is thought to be central to diabetic cataracts, retinopathy, nephropathy and neuropathy [5].

Studies on various organisms have primarily focused on using aldose reductase inhibitors (ARIs) to counter AR activation. These inhibitors will seek to prevent the transformation of glucose to sorbitol to reduce the osmotic and oxidative stress. Nonetheless, synthetic ARIs have noted limitations such as poor efficacy, side effects, and toxicity. According to Hussain et al. (2020), such limitations have led to new trends in the search for naturally derived AROMA with better safety profile and pharmacological acceptability [6]. Among these, flavonoids naturally occurring polyphenolic compounds are especially promising due to their structural flexibility and affinity for interaction with the AR active site through different modes of interaction such as hydrogen bonding, hydrogen bond acceptor interactions, hydrophobic interaction and π-π stacking interactions.

*E. pulcherrima*Willd Ex Koltz, or poinsettia, is a shrub used for centuries in folk medicine. According to researchers, some therapeutic uses include pain relievers, sedative potential, inflammation reducer, microbial control and antioxidants. Further studies by Khan et al. 2021 [7]; Basnett et al., 2023 [8]; Aljohani et al., 2022 [9] have corroborated these facts but suggested that the application of the plant as a source of inhibitors of AR is not thoroughly investigated. The flavonoids found in *E. pulcherrima* contain hydroxyl groups and conjugated double bonds, which are ideal for their interaction with AR and, therefore, serve as potential agents to combat the adverse effects of the polyol pathway [10]. Targeting the polyol pathway represents a promising therapeutic strategy, given the harmful effects of AR overactivation in hyperglycemia on cells at the biochemical and structural levels. Such insights show why identifying natural compounds that could potentially inhibit AR is required to address the above complications systematically [11]. Molecular docking analysis provides the rational basis for evaluating the potential of potential inhibitors and target enzymes. These Computational docking studies provide quantitative assessments of binding affinity, conformational stability, and molecular interaction dynamics. For this reason, a combination of molecular docking with in vitro biochemical assays enables researchers to verify the inhibitory properties of compounds and gain further insights into the compounds' action profile [12].

This research extracts flavonoids from *E. pulcherrima*; the ability to inhibit aldose reductase is also examined. Additionally, molecular docking simulations will provide further in-depth experimental investigations of the interactions between flavonoids and AR. By combining these approaches, this research aims to evaluate the potential benefits of E. pulcherrima flavonoids for treating diabetes complications.

These results of this study will explore the pharmacological potential of *E. pulcherrima* for the development of naturalproducts based therapies for complications resulting from diabetes.

2. Materials and methods

2.1. General

The melting points of the isolated flavonoids (**1** &**2**) were determined using a BioCote melting point apparatus. UV spectra were recorded using a UV–Visible spectrophotometer (Hitachi U-3200). IR spectra were obtained on a Nicolet 380 FT-IR spectrometer (Thermo Scientific).^{13C}NMR (150 MHz) and ^{1H}NMR (600 MHz) spectra were recorded using a Bruker Avance AV-600 cryoprobe NMR spectrometer. Electron ionization mass spectra (EI-MS) were obtained using a JEOL JMS 600 H mass spectrometer. Column chromatography was carried out using silica gel 60 (particle size 0.062–0.200 mm; Merck).

2.1. Plant collection

The*E. pulcherrima* bark, measuring between 2.5–3.5 cm,was collected in August 2018 from the University of Peshawar, Khyber Pakhtunkhwa, Pakistan. Dr. Barkatullah, a professor of the Department of Botany at the University of Peshawar, Pakistan, did the botanical identification and subsequent authentication of the plant species. The collected samples were thoroughly washed and cleaned with distilled water. Subsequently, the barks were shade dried for three days to prevent the loss of their bioactivity and then ground into fine powders. For documentation, records, and future identification, a voucher specimen with reference number PUP545 was preserved in the herbarium of the Department of Botany, University of Peshawar.

2.2. Extraction and isolation

The powdered plant materials (9.3 Kg) were subjected to cold extraction with methanol, a polar solvent, to ensure efficient extraction of bioactive compounds [13]. For this purpose, 100 liters of methanol were employed, yielding a dilute methanolic extract, which was subsequently concentrated under reduced pressure using rotary evaporation. This process produced a concentrated crude extract weighing 170.54 g. The crude extract was partitioned using solvents of varying polarity to purify further and isolate compounds. Sequential extractions were performed with n-hexane (10 L), chloroform (12 L), ethyl acetate (8 L), and 1-butanol (8 L). Among these, the methanolic fraction, weighing 34.2 g, was identified as the most promising based on its rich profile of compounds observed through thin-layer chromatography (TLC). Approximately 20 g of the methanolic fraction was subjected to silica gel column chromatography (CC), employing a gradient elution solvent system of chloroform and methanol (starting from 100:0 and gradually shifting to 0:100). This process resulted in 80 sub-fractions, designated as Fr-1 to Fr-80, based on their distinct TLC profiles. Defatting was performed by initial elution with 100 mL of n-hexane to remove non-polar impurities. Subsequently, a solvent gradient of chloroform and methanol (100:0 to 30:80) was used to isolate a sub-fraction characterized by a distinct brown colour. This sub-fraction underwent further purification through preparative chromatography using an optimized solvent system of chloroform and methanol (60:40), which yielded two bioactive compounds, which are compounds **1** (Yield = 0.47 g) and compound **2** (Yield = 0.51 g).

Only two flavonoids were isolated and characterized from a major representation in the most active chloroform fraction as well as a predominant TLC profile, namely; 5,7,8,3′,4′-pentahydroxy-3- methoxyflavone (compound **1;** m.p. = 256- 257) and kaempferol-3-β-D glucopyranosyl (**2**; m.*p* = 176–178). Some of the other small secondary metabolites in low yield subfractions were observed, but they were also

not purified because of their minimal quantities, as well as a narrow scope of the present study, which was particularly aimed at the isolation of such major bioactive compounds. The chemical structures of compounds **1** and **2** (Fig. 1), was elucidated by comparing the physical and spectroscopical data with previously reported data [14,15]

2.3. Aldose reeducates inhibitory activity

The aldose reductase inhibitory assay was carried out according to the method described by Imran et al. (2022)[16], which was based on the ability of the test compounds to inhibit the enzyme by a standard procedure. The reaction mixture was made to a volume of 100 μL, and it contained several essential constituents. These comprised 20 μL of 100 mM sodium phosphate buffer at pH 6.2 for optimal enzymatic activity, 30 μL of bovine aldose reductase enzyme, diluted to 20 μL of the substrate DL-glyceraldehyde at a concentration of 10 mM and finally, 20 μL of 0.1 mM NADPH as a coenzyme. Furthermore, the compound under-tested was added into the mixture by 10 μL with the final soluble concentration up to 0.2 mM.As a beginning step of the whole assay, the reaction mixture was warmed at 32 °C for 10 min without NADPH to minimize the initial enzymatic activity. It was then activated with NADPH, and the flow of the enzymatic activity was monitored for 5 min. This structure enabled closely supervising the enzyme's behavior and relationship with the test compounds. d-saccharic acid 1,4-lactone was used as a reference standard, and its result was used to set a standard for evaluating the inhibitory potency of the test compounds.

Aldose reductase 1 (ALR1) enzyme from bovine lens (Sigma-Aldrich) was used in the assay.This type of enzymes align to the isoform tested through molecular docking, meaning that the experimental process is consistent and also relevant. ALR1 was chosen because it is available in the purified form and is reported to be structurally homologous to human ALR1. However, we recognize the significance of the ALR2 in the diabetic complications. Now we explain in the rewritten Discussion that comparison with ALR2 will be carried out in future work to have a better understanding of isoform selectivity.

Therefore, the assay output of the work was the IC_{50} values of the compounds obtained according to the generally amplified protocols, thus finding out the concentration of each compound, which could give 50 % inhibition of aldose reductase activity. This procedure also allowed the assessment of the inhibitory capability and, equally important, provided an objective and accurate method of selecting the most Aldose Reductase inhibitory compounds. The ability to screen any potential therapeutic agents in their own right is this study's strength; that makes it relevant in looking for ways to manage diabetes-associated complications for which aldose reductase inhibition is central.

2.4. Statistical analysis

Statistical analysis was carried out, and the results were presented in SEM.

2.5. Computational chemogenomic analysis

Computational chemogenomic analysis was performed through PIDGIN chemogenomic software v.2 to investigate the potential targets for the isolates of *E. pulcherrima.* The SMILES of the isolates were used as input files for the analysis. The current study incorporated the following "*python predict_per_comp.py input.csv 30 0.5 0.3 "Homo sapiens (Human)"*", Python-based script, resulting in binary prediction (0=inactive; 1=active) [17,18]. The hashed Extended Connectivity Fingerprint (ECFP_4) and circular Morgan fingerprints (radius=2, length=2048 bits as input vectors for models) were generated using RDKit [19]. The optimization of the models was done using binary features for active and inactive compounds, followed by the generation of the probability ratio. Thereby, predicting the binding probability between the isolates and the receptor. Finally, the optimized cut-off values for each target were set, and the probability values were converted into binary prediction [20].

2.6Target. Protein retrieval

The crystallographic structure of potential target aldose reductase (ALR1) was retrieved from the protein data bank (PDB ID: 4QX4). The crystal structure of ALR1 belongs to the *Homo sapiens* and is categorized as oxidoreductase family. Additionally, the protein consists of an alpha chain with a sequence length of 316 amino acids. The crystal structure was resolved at 1.26Å and downloaded in PDB format. Furthermore, a native co-crystal ligand (CCL) 3E2 also resides within the catalytic site of the target receptor [21].

2.7. Ligands retrieval and preparation

The structures of isolates of *E. pulcherrima* were drawn on ChemDraw Professional 16.0 to obtain their 2D and 3D conformations. The 3D structures were further saved in SDF format for ligand preparation additionally, the CCL, PubChem CID: 685,919, was also saved in SDF format and then imported to the Maestro workspace of Schrodinger 2020–3v12.5. The LigPrep tool was used to obtain the conformational optimization of these ligands. Epik module was selected for ionization of the compounds at pH = 7.0 ± 2, followed by desalting and tautomerization. Additionally, specific chiralities were retained to mitigate stereoisomerism, followed by generating 32 possible poses for each compound. Finally, a force field of OPLS3e was applied for optimization and energy-minimization of these compounds [22].

2.8. Protein preparation

The crystallographic structure of the target protein ALR1 was subjected to the Maestro workspace of Schrodinger 2020–3v12.5 for optimization and energy minimization through the Protein Preparation Wizard tool. Initially, the crystallographic structure of the target protein was preprocessed by assigning bond order and adding hydrogen bond (H-bond), subsequently followed by the generation of zero-order bonds for metals and bridging the gap between missing loops and side chains by applying the prime job under Epik module at pH of 7.0 ± 2. Additionally, PROPKA was applied at a pH of 7.0 for H-bond optimization, followed by the removal of water molecules beyond 3.0Å Finally, heavy atom RMSD was converged to 0.30Å to minimize the crystal structures under the applied force field of OPLS3e [22,23]. Afterward, a grid was

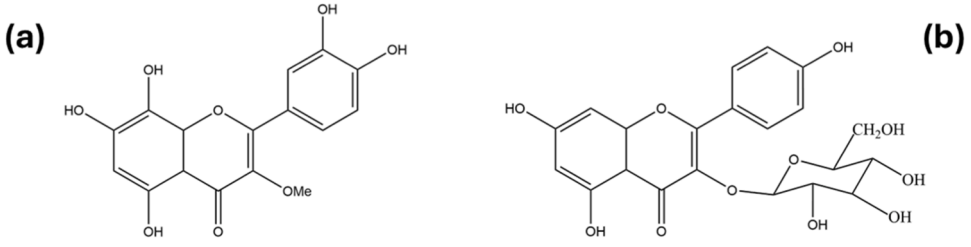

Fig. 1. Chemical Structures of Flavonoids compound 1 (a) and compound (2) (b) Isolated from E. pulcherrima.

generated using the GLIDE suite of Schrodinger 2020–3v.12.5. The receptor grid was generated within the centroid cavity of CCL for efficient binding interactions between the compound and the active residues of the binding pocket of the target receptor [24]. Additionally, a grid was also generated around the active residues of the binding site to ensure biologically relevant interactions with the compounds, accounting for receptor flexibility.

2.9. Molecular docking studies

The molecular docking was conducted on the Ligand docking suite of Schrodinger 2020–3v.12.5 using XP (extra precision) mode for flexible ligand sampling. Both energy-minimized files of receptor and ligands were subjected to the Maestro workspace, and the root mean square deviation (RMSD) value was computed for input ligand geometries to validate the accuracy of the docking protocol [25]. Molecular docking allows us to investigate the binding affinity between the compounds and the target receptor ALR1 in terms of d-scores (docking scores). Furthermore, the docked complexes were visualized on Discovery Studio Visualizer and PyMol Molecular Graphics System to analyze the binding interactions. Furthermore, to enhance the biological relevance of the docking results, a similar docking protocol was also carried out within the grid generated for predefined active site residues of the target protein ALR1.

2.10. ADME analysis

The pharmacological assessment of the isolates of *E. pulcherrima* was investigated on SwissADME, a web server. This server applies the molecular fingerprinting metrics to assess the absorption, distribution, metabolism, and excretion (ADME) across various descriptors. The canonical SMILES of the isolates were subjected to the query box as input data to evaluate ADME [26].

2.11. Toxicity prediction

The toxicity prediction of the isolates of *E. pulcherrima* was predicted on a machine learning application, i.e., StopTox, to assess the potential toxicity on immediate exposure to the compound. The in vivo assays, referred to as the "6-Pack," were employed on models to predict the acute oral, dermal, and inhalation toxicity as well as skin sensitization, irritation and corrosion of skin, and eye irritation and corrosion of the compounds. The canonical SMILES of the isolates were subjected to the query box as input data to predict acute toxicity [27].

2.12. Bioactivity assessment

The potential pharmacological targets for the isolates of *E. pulcherrima* were screened on a web server. i.e., PASS (prediction of activity spectra for substances). The canonical SMILES of the isolates were subjected to the query box as input data for screening of pharmacological targets. Resultantly, the output data was retrieved as Pa (probability for active compound) and Pi (probability for inactive compound), based on structural activity relationship (SAR) [28].

2.13. Density functional theory (DFT) studies

The isolates of *E. pulcherrima* were imported to Gauss View software v.5.0.8 for DFT analysis. The Gaussian 09 W program was used to generate optimized structural geometries for investigating the chemical reactivity of the compounds. The current study applied Becke's 3-parameter Lee-Yang-Parr (B3LYP) method with a basis set of $6–311^{++}G$ in the physiological phase, employing a conductor-like polarizable continuum model (CPCM) [29]. The frontier molecular orbitals (FMOs) were computed through the DFT approach and viewed on Gauss View software v.5.0.8. In addition, global reactivity descriptors were computed by applying Koopman's theorem, using the following listed equations[30]:

$$\text{EnergyGap}\left(\Delta E_{Gap}\right) = E_{LUMO} - E_{HOMO} \quad (1)$$

$$\text{Electronegativity}\chi = -1/2(E_{HOMO} + E_{LUMO}) \quad (2)$$

$$\text{ElectrochemicalPotential}\mu = 1/2(E_{HOMO} + E_{LUMO}) \quad (3)$$

$$\text{ChemicalHardness}\eta = 1/2(E_{LUMO} - - E_{HOMO}) \quad (4)$$

$$\text{ChemicalSoftness}\, S = 1/2\eta \quad (5)$$

$$\text{Electrophilicity}\omega = \mu^2/2\eta \quad (6)$$

$$\text{IonizationPotential}\, I = - - E_{HOMO} \quad (7)$$

$$\text{ElectronAffinity}\, A = - - E_{LOMO} \quad (8)$$

Moreover, the molecular electrostatic potential surface (MESP) mapping was generated over the compounds to gain insight into the overall charge distribution. The checkpoint file (.chk*) of the compounds, generated through the Gaussian 09 W program, was utilized to create MEPS and viewed on Gauss View software v.5.0.8.

2.14. Molecular dynamics (MD) simulations

MD simulations were performed for 250 ns on Desmond, a suite from Schrodinger, to gain deep insight into the conformational stability of the protein-ligand complex in a real-time setting by incorporating Newton's classical equation of motion [31,32]. Initially, both the protein and ligands were optimized and minimized using the Protein Preparation Wizard tool from Schrodinger, followed by the elimination of steric clashes and aberrant geometries. The system was built using the System Builder tool, and the Intermolecular Interaction Potential 3 Points Transferable (TIP3P) solvent model was applied, generating an orthorhombic box under the OPLS_2005 force field [33]. Additionally, counter ions and 0.15 M NaCl were added to neutralize and simulate a normal physiological environment for the complex, maintaining a temperature of 300 K and pressure of 1 atm throughout the 250 ns simulation trajectory. The generated trajectories were stored every 100 ps for inspection, and complex stability was evaluated by root-mean-square deviation (RMSD), root-mean-square fluctuation (RMSF), radius of gyration (ROG), and the number of hydrogen bonds. Moreover, the principal component analysis (PCA) and dynamic cross-correlation matrix (DCCM) analysis were also performed through the Bio3D package of R, in R scripted language [34,35].

2. 15Molecular mechanics and generalized born surface area (MM-GBSA) calculations

The binding free energy (Gbind) of the complexes during MD simulations was calculated through the MM-GBSA module of Prime. The Gbind was calculated by applying below-mentioned equation, using the VSGB solvent model and rotamer techniques under a force field of OPLS_2005.

$$\text{dGbind} = G_{complex} - -\left(G_{protein} + G_{ligand}\right) \quad (9)$$

dGbind = binding free energy, $G_{complex}$ = free energy of the complex, $G_{protein}$= free energy of the target protein, and G_{ligand} = free energy of the ligand.

3. Results

3.1. In vitro analysis

3.1.1. Aldose reeducates inhibitory effects

The inhibitory activity for aldose reductase in the flavonoids isolated from *E. pulcherrima* indicated moderate to excellent inhibitory activity, as presented in Table 1. Moderate inhibition was recorded with the crude methanolic extract at 0.2 µg concentration, i.e., 64.39 % inhibitionwith an IC_{50} 4.23 ± 1.09 µg. However, the free flavonoids demonstrated markedly improved activity when tested individually. Compound **1** showed dose-dependent inhibition, reaching 84.02 % at 0.2 µM, with an IC50 of 0.97 ± 0.53 µM. Likewise, Compound **2** also demonstrated a high activity level; its inhibition reached 86.09 % at the same concentration level with an IC_{50} of 0.92 ± 0.48 µM.

The standard inhibitor, d-Saccharic acid 1,4-lactone, had the best result, 89.63 % inhibition, and the IC_{50} value was 0.88±0.34 µM. The inhibitory effect of identified flavonoids, specifically Compound **1** and Compound **2**, has established a highly significant aldose reductase inhibitory activity, which indicates the possibility of these natural compounds as potential therapeutic sources for preventing diabetic complications arising due to aldose reductase activity. This study also strengthens the possibility of using *E. pulcherrima* as a source of bioactive molecules for diabetes control.

3.2. In silico analysis

The chemogenomic analysis revealed ALR1 as a potential active target for the isolates of *E. pulcherrima* to inhibit aldose reductase activity. The target protein ALR1, shown in **Figure S1**, was docked with the isolates illustrated in **Table S1 (**See supplementary file**)**, representing the 2D, 3D,and their SMILES ID conformations of the compounds.

3.2.1. Molecular docking studies

The docking studies were executed on Schrodinger 2020–3v.12.5 showed the binding affinity between the target receptor ALR1 and the isolates of *E. pulcherrima*. The docking scores illustrated in Table 2 revealed that both isolates stood out as top-scoring compounds in comparison to CCL, which possessed the lowest docking score among the three. The high docking scores of both isolates indicated strong binding affinity with the ALR1 receptor, suggesting their significant inhibitory potential for therapeutic purposes. The obtained docking results were verified by calculating the RMSD value of native CCL with the docked pose, which resulted in <2.0Å(Table 2). The computed RMSD value verified the accuracy of the docking protocol.

Moreover, the docking performed on predefined active site residues illustrated in **Table S2 (**See supplemntry file**)**, showed compound 1 (−6.697 kcal/mol) possesseda higher docking score, as compared to compound 2 (−4.651 kcal/mol). This also underscores a higherbinding efficiency and potent inhibitory activity for compound 1 against ALR1 protein. The docking scores are presented in **Table S3 (**See supplemntry file**)**.

3.2.2. Visualization and interaction analysis

The 2D and 3D binding interactions were visualized on Discovery Studio Visualizer and PyMol molecular graphic systems, respectively, shown in Fig. 2. The interaction analysis of CCL with ALR1 revealed the formation of favorable conventional H-bond with hydroxyl and carbonyl groups by following residues Trp111, Tyr48, and His110 at a distance of 2.00Å, 2.02Å, and 1.86Å, respectively. Additionally, water-mediated interaction was also observed by HOH 819 residue of the alpha chain at a distance of 3.02Å Further, strong electrostatic interactions were formed with the hydroxyl group of the CCL at a range of 5.93Å and 5.36Å with Trp20 and Lys77 residues, respectively. These interactions significantly contributed to stabilizing the ligand within the binding cavity of target receptor ALR1. Additionally, the hydrophobic interactions also contributed to implying strong binding affinity by the formation of mixed π-alkyl interactions.

Contrastingly, compound 1 showed significant polar and non-polar interactions, indicating its inhibitory potential against the ALR1 receptor. The formation of polar interactions including H-bond signifies the polarity of the complex. Various types of H-bonds encompassing classical, non-classical, and water-mediated bonds were observed specifically with the hydroxyl and carbonyl group of the compound. The key residue HOH819, involved in CCL, was also engaged in the formation of water-mediated interactions close to the compound (i.e., 2.40Å). However, the conventional H-bonds were formed at a distance of 2.62Å, 2.74Å, 2.04Å, and 2.93Å by the following residues of alpha chain: Leu300, Asn160, and Gln183, respectively. The favorable polar interactions enhanced the polarity as well as stability of the docked complex. Additionally, strong electrostatic charged interaction was visualized by Trp219 residue at a range of 3.99Å, and non-polar hydrophobic bonds were formed,contributing to balance the hydrophobicity of the binding pocket, ultimately stabilizing the compound within the cavity.

Similarly, the compound2 formed only two types of interactions with the binding cavity residues of ALR1, i.e., favorable polar H-bond and non-polar hydrophobic bonds. The stability of the docked complex was mainly enhanced by H-bond formation with hydroxyl and carbonyl groups of the compound. The following residues of the binding cavity: Val47, Tyr48, Lys21, Trp20, and His110 were responsible for polar interactions at specified distances, shown in Fig. 2. Whereas π-hydrophobic interactions were formed by Phe122, further stabilizing the compound within the binding cavity of the target receptor ALR1.

On the other hand, the binding interaction with the active site residues, shown in **Figure S2,3**, revealed that compound 1 established significant hydrophobic interactions with the key residues of the active site i.e., Tp219, Cys298, Ala299, Leu300, and Leu301, when exposed to the allosteric site of target protein ALR1. Notably, conventional H-bonds were also formed with Val297, Ala299, and Cys298 residues of alpha chain of ALR1 protein, highlighting the stable and specific interaction pattern. Likewise, compound 2 also formed non-covalent hydrophobic interactions upon exposure to the allosteric site of protein reinforcing the notion of structurally adaptive involvement. Overall, these interaction analyses indicated that compound 1 was well bound showing localized conformational flexibility of the target protein ALR1. These interactions also suggested the structural compatibility of the both compound 1 and 2 with the dynamic binding environment of ALR1.

3.2.3. Surface mapping

The binding interactions of isolates of *E. pulcherrima* were further analyzed thoroughly by displaying receptor surfaces through Discovery

Table 1
Aldose Reductase Inhibitory activity of flavonoids isolated from E. pulcherrima.

Sample	Concentration	% inhibition	IC_{50} ±SEM (µM)
Extract	0.2 µg	64.39	4.23±1.09
Compound 1	0.2 µM	84.02	0.97±0.53
Compound 2	0.2 µM	86.09	0.92±0.48
D-Saccharic acid 1, 4-lactone	0.2 µM	89.63	0.88±0.34

Table 2
Docking scores of isolates of E. pulcherrima against target protein ALR1 (PDB ID: 4QX4) in comparison to CCL (3E2).

Target Proteins	PDB ID	Docking Scores (kcal/mol)			RMSD Value Å
		CCL	Compound 1	Compound 2	
ALR1	4QX4	−7.238	−9.629	−10.248	0.08441

*RMSD: root mean square deviation.

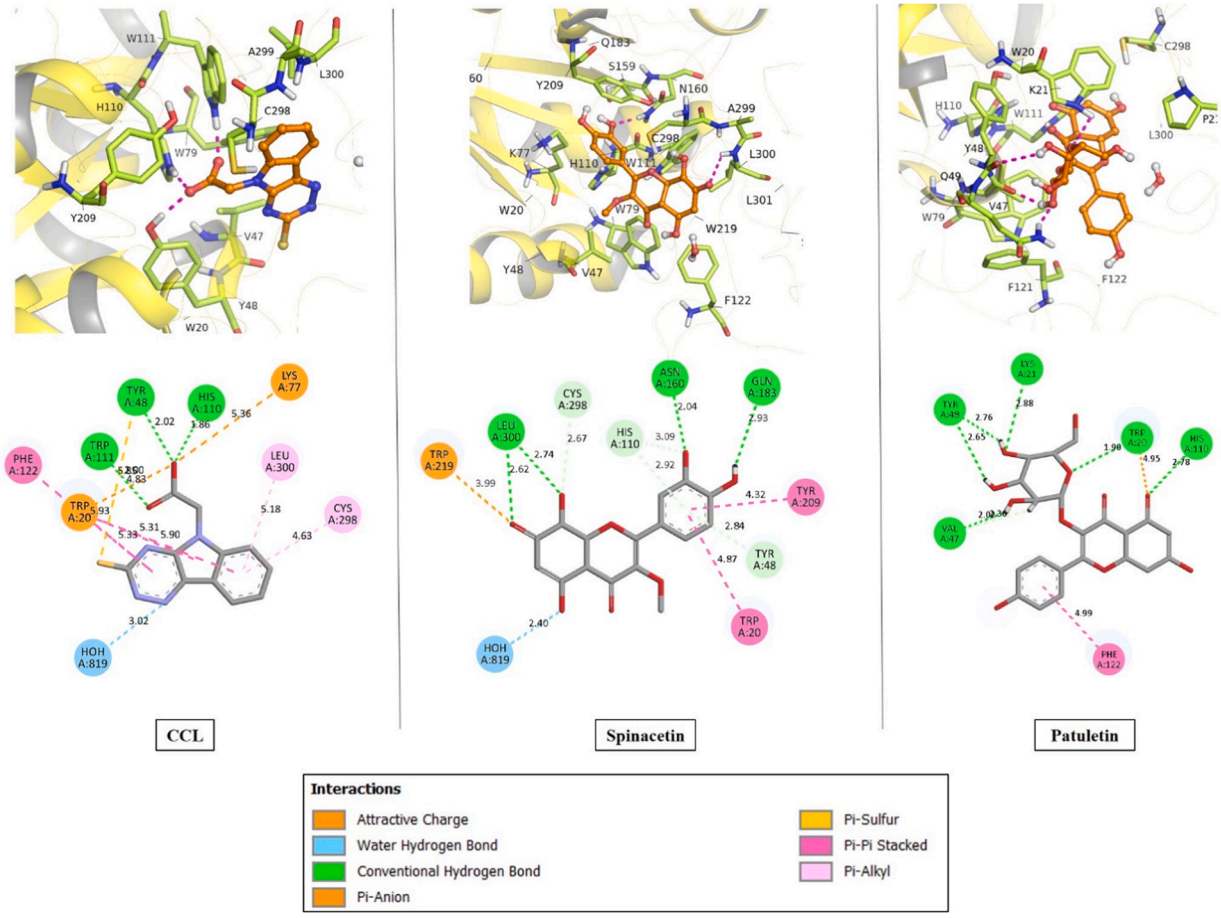

Fig. 2. 2D & 3D binding interactions pattern of isolates of E. pulcherrima, in comparison to CCL (3E2), viewed on Discovery Studio Visualizer and PyMol Molecular Graphic System, respectively.

Studio Visualizer, shown in Fig. 3. The figure illustrated solvent accessible surface area (SAS), H-bond, and hydrophobicity. The SAS of compound 2 (A) and compound 1 (D) revealed strong binding affinity and interactions with the active site residues as this region was less solvent-accessible, suggesting the inhibitory affinity within the receptor. The hydrophobic surface mapping of compound 1 (E) was more pronounced than compound 2 (B), reflecting the stability and inhibitory potential of compound 1 within the binding pocket. Finally, the H-bond surface mapping of compound 2 (C) highlighted that the polar H-bonds formed by the residues acted as both donors and acceptors with hydroxyl and carbonyl groups. Conversely, compound 1 (F) possessed a more pronounced region for H-bond donors with the residues of the active site. The significant polar and non-polar interactions suggested a suitable inhibitory potential of the compounds against ALR1 for therapeutic purposes.

3.3. ADME analysis

The molecular fingerprinting approach evaluated the ADME properties of the isolates of *E. pulcherrima* across various descriptors encompassing physiochemical features, lipophilicity, solubility, medicinal chemistry, drug-likeness, and pharmacokinetics, highlighted in Table 3.

The physiochemical features revealed that compound 1 followed all rules defined by Lipinski, referred to as Lipinski's rule of five (LRF). Whereas compound 2 violated LRF by exhibiting >10 H-bond acceptors and >5 H-bond donors. Moreover, the total polar surface area (TPSA) also exceeded >140Å^2, indicating poor membrane permeability as well as poor oral bioavailability. The lipophilicity measured across Log $P_{o/w}$ (octanal-water partition coefficient) and solubility measured across Log S revealed that both compounds showed balanced hydrophilicity and lipophilicity, indicating their potential for therapeutic purposes. Subsequently, the medicinal chemistry revealed that compound 2 was devoid of any PAINS and Brenk alert, while compound 1 was observed to have both types of alerts, indicating potential assay interference or toxicity risks. Additionally, the synthetic accessibility of compound 1 was closer to 1 than compound 2, indicating the synthetic feasibility of compound 1. Moreover, the drug-likeness of the compounds was evaluated across various rules defined by Lipinski, Ghose, Veber, and Muegge. The results illustrated in Table 3 showed that compound 1 was suggested to be a drug-like compound, while compound 2 showed violations against all rules, indicating that compound 2 could not be considered a promising drug-like candidate. Finally, the pharmacokinetics analysis revealed that compound 1 showed high gastrointestinal (GI) permeability while compound 2 possessed low GI permeability. The low GI absorption of compound 2 was mainly affected by the high TPSA value. However, the metabolism evaluated across the cytochrome P450 (CYP-450) family revealed that both compounds were not involved in any potential drug-drug interactions

3.3.1. Oral bioavailability

One of the important parameters in pharmacological evaluation is the oral bioavailability of the compound. The oral bioavailability of the isolates of *E. pulcherrima*shown in Fig. 4, revealed that compound 1 showed acceptable oral bioavailability, as all the descriptors were marked within the red zone of the radar chart. Similarly, the bioavailability score of compound 1 was also 0.56 compared to compound 2, which scored 0.11. A pronounced fluctuation in the polarity of

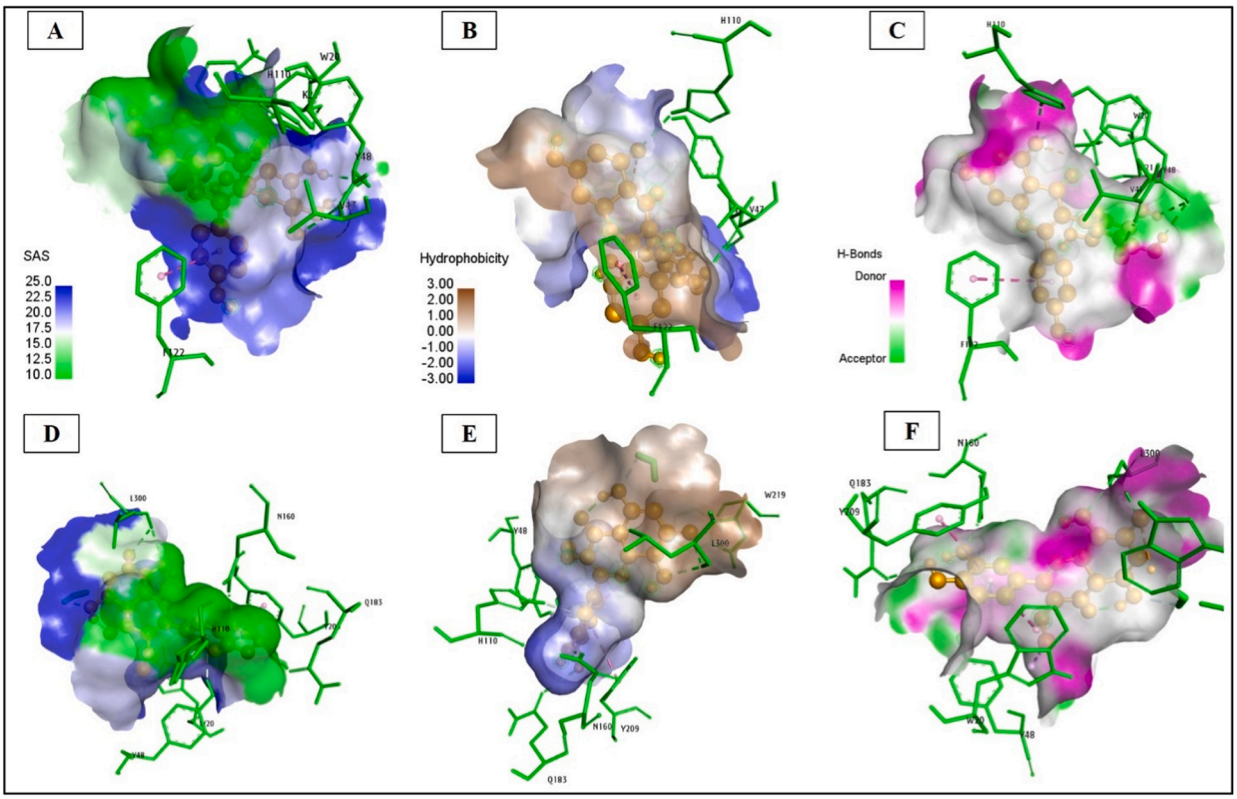

Fig. 3. Display of receptor surface over isolates of E. pulcherrima, assessed through Discovery Studio Visualizer. (A, B, C: Compound 2& D, E, F: compound 1). SAS: solvent accessbile surface.

Table 3
ADME evaluation of isolates of E. pulcherrima measured across various descriptors, assessed through SwissADME.

Physiochemical Properties						
Code	Molecular weight (g/mol)	No. of heavy atoms	No. of rotatable bonds	H-bond acceptors	H-bond donors	TPSA (Å^2)
1	334.28	24	2	8	5	136.68
2	450.39	6	4	11	7	186.37
Lipophilicity						
Code	Log $P_{o/w}$ (iLOGP)	Log $P_{o/w}$ (XLOGP3)	Log $P_{o/w}$ (WLOGP)	Log $P_{o/w}$ (MLOGP)	Log $P_{o/w}$ (SILICOS-IT)	Consensus Log $P_{o/w}$
1	1.62	0.41	1.78	−1.98	−0.10	0.35
2	1.09	−0.73	−0.64	−2.99	−1.79	−1.01
Water solubility and Medicinal Chemistry						
Code	Log S (ESOL)	Log S (Ali)	Log S (SILICOS-IT)	PAINS	Brenk	Synthetic accessibility
1	−2.22	−2.85	−0.98	1	1	4.63
2	−2.05	−2.71	0.49	0	0	5.88
Drug-likeness						
Code	Lipinski	Ghose	Veber	Muegge	Bioavailability score	
1	Yes	Yes	Yes	Yes	0.56	
2	No	No	No	No	0.11	
Pharmacokinetics						
code	GI absorption	BBB permeant	CYP1A2 inhibitor	CYP2C19 inhibitor	CYP2C9 inhibitor	CYP2D6 inhibitor	CYP3A4 inhibitor
1	High	No	No	No	No	No	No
2	Low	No	No	No	No	No	No

*TPSA: total polar surface area; PAINS: pan assay interference compound; GI: gastrointestinal; BBB: blood-brain barrier.

compound 2 that was marked outside the zone also suggested a high level of TPSA. Overall, compound **1** stood out as a suitable compound with promising oral bioavailability for therapeutic purposes.

3.4. Toxicity prediction

The predicted acute toxicity of the isolates of *E. pulcherrima,*represented in Fig. 5, showed that both compounds showed no potential harm on immediate exposure with a confidence rate of greater than and equal to 54 % across all parameters. However, both isolates showed acute dermal toxicity with confidence rates of 64.0 % (compound 1) and 51.0 % (compound **2**), indicating potential harm upon dermal contact. Notably, the toxicophore domains highlighted in red color could be considered hotspot sites for structural modification to reduce toxicity.

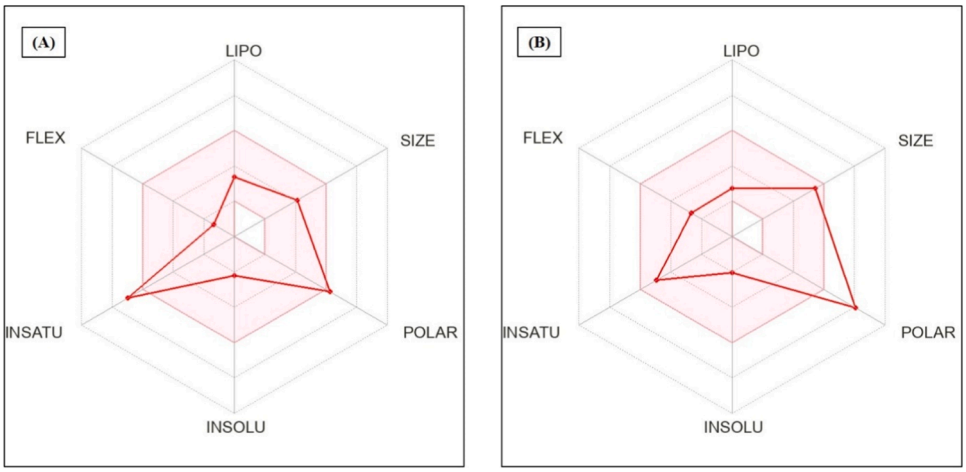

Fig. 4. Radar chart showing normal physiochemical space for oral bioavailability of isolates of E. pulcherrima, assessed through SwissADME. (A) compound 1(B) compound 2. FLEX: flexibility; LIPO: lipophilicity; POLAR: polarity; INSOLU: insolubility; INSATU: insaturation.

3.5. Bioactivity assessment

The bioactivity of the isolates of *E. pulcherrima* was assessed through PASS online, as presented in Table 4. The results highlighted that compound 1 stood out with the highest active status across all investigated assays, with a probability score of 65.3 %. Comparatively, the other compound, compound 2, exhibited a lower probability index across a majority of the biological assays listed in Table 4. However, the antineoplastic and membrane permeability inhibitor showed higher probable activity with compound 2 (i.e.,> 90 %) compared to compound 1. The overall bioactivity assessment suggested a promising probable activity of compound 1 for therapeutic purposes.

3.6. DFT studies

The DFT studies carried out on the Gaussian 09 W program calculated the FMOs values illustrated in Table 5. The difference between FMOs(Fig. 6), referred to as the energy gap, showed that compound 1exhibited the smallest energy gap, followed by CCL and compound 2. The energy gap indicated that compound 1 possessed the highest reactivity due to a small energy gap, whereas compound 2 exhibited high stability and less reactivity due to a large energy gap. The FMO calculations suggested that compound 1 could interact effectively with the target receptor ALR1.

Koopman's theorem was applied to gain more insight into the global reactivity descriptors of both compounds. The results illustrated in Table 5 showed that the CCL possessed a higher ionization potential, followed by compound 2 and compound 1, respectively. On the other hand, electron affinity revealed the chronologically increasing values as CCL >compound 1>compound 2. These results indicated that CCL was more electrophilic, while compound 1 showed a moderately balanced electron affinity. The electronegativity and electrochemical potential also showed a chronological increase in values in the following order: CCL >compound 2>compound 1. Contrastingly, the electrophilicity showed that compound **2** possessed the lowest electrophilicity, while compound 1 showed moderate electrophilicity, making it a suitable candidate for nucleophilic reactions. Furthermore, the softness was inversely associated with the chemical hardness, highlighting that the hardness of CCL and compound **2** was also higher than compound **1**, indicating their lower reactivity.

The molecular electrostatic potential (MESP) surface mapping shown in Fig. 6 represents the charge distribution within the compounds. The positive electrostatic potential of the compounds was highlighted as red domain, indicating electron-deficient regions, while the negative potential was highlighted as blue domains, indicating electron-rich regions within the compounds. The surface mapping of CCL showed a pronounced positive electrostatic potential around polar functional groups, suggesting a suitable site for conventional H-bond interactions. In contrast, compound **2** showed a balance between electrophilic and nucleophilic reactions. Notably, positive electrostatic potential was observed near hydroxyl and carbonyl groups, suggesting its enhanced binding affinity than other compounds. Finally, compound 1 also possessed both electrophilic and nucleophilic regions with a more pronounced positive electrostatic potential, particularly around the hydroxyl group.

3.7. MD simulations

The MD simulations carried out on 250 ns revealed significant insight into the structural stability and binding interactions between the target protein ALR1 and the ligands. The plot shown in Fig. 7 portrays the RMSD, RMSF, ROG, and total number of the H-bond profiles of both CCL and compound 1 complexed with the target protein. Additionally, the conformational changes within the structure during simulations after a few ns intervals are presented in **Figure S4**.

The RMSD plot revealed that the CCL complex attain equilibrium after 50 ns, whereas compound 1 complex slightly fluctuates in the initial phase and maintains equilibrium after about 100 ns. Moreover, the compound 1 complex (~1.5–2.2 Å) exhibited a slightly lower RMSD value compared to the CCL complex (~1.8–2.3 Å). Notably, the RMSD values for both compounds ranged <3 Å, indicating enhanced structural stability upon ligand binding.

The RMSF plots showed that compound 1 complex exhibited flexibility in the loop regions, particularly around 120–140 and 210–230 residues of the alpha chain of the target protein. Contrastingly, almost similar but slightly more pronounced fluctuation pattern was observed in the loop regions of the CCL complex, specifically around 120–130 and 210–230 residues. The RMSF highlighted that the fluctuation pattern of compound 1 indicated slightly localized rigidity, stabilized regions that were more dynamic in unbounded protein, underscoring overall stability of the compound 1 complex under real-time settings.

The ROG analysis remained constant at around ~19.2–19.6 Å for both CCL and compound 1 complexes. This indicated that both structures maintained compactness throughout 250 ns simulation trajectory. Therefore, demonstrating the structural integrity of the protein and reflecting a well-folded structure of the target protein.

The H-bond analysis demonstrated a slight initial fluctuation, which stabilized and formed consistent H-bonds around 50–110 for compound 1 with the target protein throughout the trajectory. Conversely, CCL also formed H-bonds (~150–250), thereby stabilizing the docked complex.

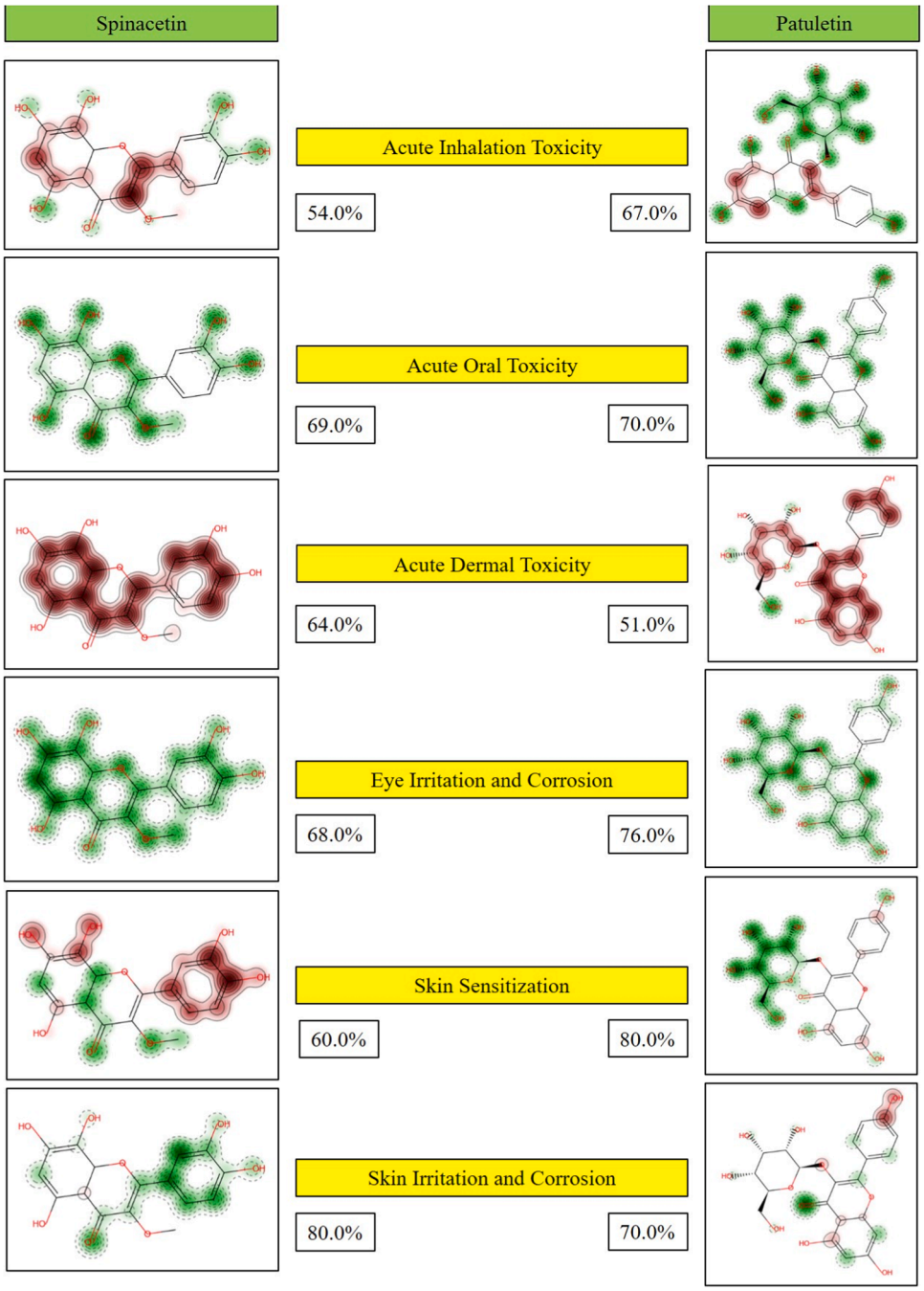

Fig. 5. Acute Toxicity Prediction of isolates of E. pulcherrima, assessed through StopTox.

Table 4
Bioactivity assessment of potential biological targets for isolates of E. pulcherrima across various biological assays, assessed through PASS Online.

Biological assays	PASS Prediction			
	Compound 1		Compound 2	
	Pa	Pi	Pa	Pi
Membrane integrity agonist	0.915	0.008	0.964	0.003
Antineoplastic	0.863	0.006	0.901	0.005
JAK2 expression inhibitor	0.754	0.012	0.232	0.192
Anti-mutagenic	0.738	0.005	0.191	0.081
Membrane permeability inhibitor	0.741	0.024	0.916	0.003
Kinase inhibitor	0.688	0.013	0.361	0.088
AR expression inhibitor	0.653	0.008	0.202	0.147

Table 5
Comparative analysis of FMOs and global reactivity descriptors among isolates of E. pulcherrima with CCL (3E2), based on Koopman's theorem.

Parameters for DFT analysis	Compound 1	Compound 2	CCL (3E2)
HOMO (a.u.)	−0.19507	−0.21548	−0.24401
LUMO (a.u.)	−0.08421	−0.07449	−0.10395
Energy Gap (ΔE_{Gap}) (eV)	3.02	3.84	3.81
Ionization Potential (I) (eV)	5.31	5.86	6.64
Electron affinity (A) (eV)	2.29	2.03	2.83
Electronegativity χ (eV)	3.80	3.95	4.73
Electrochemical potential μ (eV)	−3.80	−3.95	−4.73
Hardness η (eV)	1.51	1.92	1.91
Softness S (eV^{-1})	0.663	0.521	0.525
Electrophilicity ω (eV)	4.79	4.06	5.88

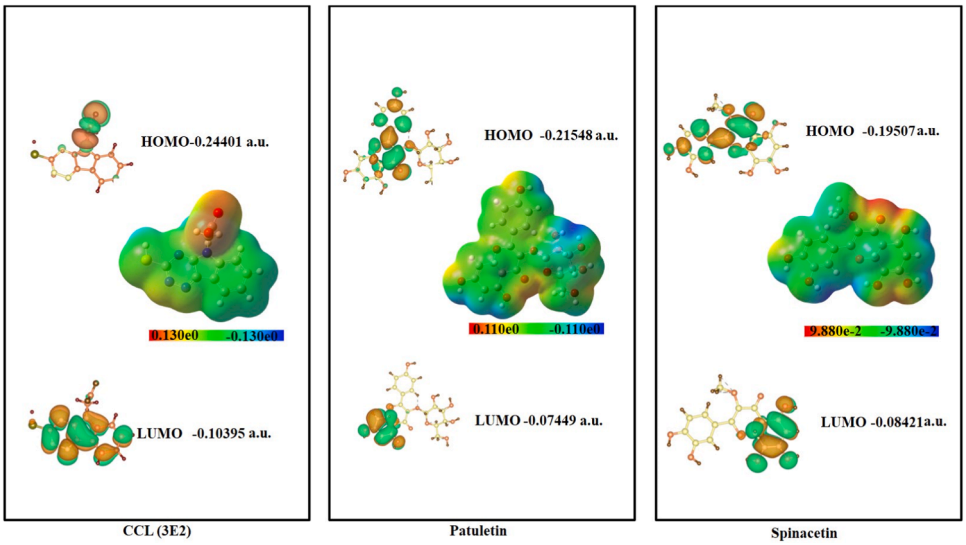

Fig. 6. Optimized structural orientation of frontier molecular orbitals and molecular electrostatic potential surface mapping of isolates of E. pulcherrimaand CCL (3E2).

These results indicated strong and favorable binding affinity for compound 1 and CCL against the target protein.

Overall, the simulation analysis underscored that compound 1 exhibited increased structural stability and moderate flexibility, highlighting a stable and favorable interactions pattern.

3.8. PCA and DCCM analysis

The PCA and DCCM graphs shown in Fig. 8, further revealed the global and local motion of docked complexes, demonstrating the conformational changes in the protein structure and internal residue communication network. The scattered plots of PCA for both complexes are illustrated as eigenvectors (PC1, PC2, and PC3) and eigenvalues. The CCL PCA plot was observed to be more scattered and dispersed in PC1 (20.56 %) and PC2 (9.78 %), indicating higher fluctuation in protein upon ligand binding. Contrastingly, the plot of compound 1 showed comparatively low variance in PC1 and PC2, indicating higher stability and strong binding affinity upon ligand binding. The scree plot also supported the PCA results, indicating more dominance of fewer PCs linked with stronger and more stable protein-ligand interactions for compound 1 (approx 41.61 %).

The DCCM analysis also measured the time-correlated motions between amino acid residues of the alpha chain throughout the 250 ns simulation trajectory, ranging from fully correlated (+1) to fully anti-correlated (−1). The DCCM analysis of CCL complex exhibited more positive and negative correlations in an off-diagonal pattern, indicating higher flexibility as observed in PCA. On the other hand, a more focused DCCM pattern was observed with fewer and localized positive and negative correlations. The localized and minimal motion of residues with compound 1 indicated more stability within the protein internal dynamics, highlighting greater binding affinity of compound 1 with the target protein.

3.9. MM-GBSA Analysis

The results of MMGBSA analysis illustrated in Table 6 provides a more detailed knowledge for binding free energies for CCL and compound 1 complexes, elucidating distinct binding mechanisms and affinities for both complexes. The results showed that compound 1 possessed significantly higher binding energy i-e., −38.458 kcal/mol than CCL, which exhibited −30.813 kcal/mol. These binding energies indicated that compound 1 binds more strongly than CCL, as observed in docking studies. The lipophilic interaction energies also demonstrated significantly higher and more favorable lipophilic contribution in compound 1 complex (−24.694 kcal/mol) rather than in the CCL complex (−9.158 kcal/mol). Whereas, in the case of vdW interactions, CCL exhibited slightly more favorable energy i-e., 27.255 kcal/mol, than compound 1 (−23.126 kcal/mol). This indicated that CCL may have more closer packing within the binding site. However, a notable difference in electrostatic interactions was observed, which suggested a major driving force of binding for the CCL within the binding site. Moreover, the H-bond contribution showed comparatively favorable interactions in both complexes, indicating the formation of a stronger H-bond with the target protein. Finally, the packing energy revealed more favorable energy for compound 1 (−0.182 kcal/mol) than the CCL (−0.027 kcal/mol), highlighting the significance of compound 1 in enhanced binding stability and specificity. Overall, the MMGBSA analysis underscores that compound 1 attainsa stronger binding affinity due to enhanced lipophilicity and packing interactions, along with the contribution from H-bond interaction.

4. Discussion

The results obtained in the present study highlight the flavonoids of *E. pulcherrima*, particularly Compound **1** and compound**2**, as potentially promising inhibitors of aldose reductase (AR), an enzyme directly linked to hyperglycemia and diabetic complications. Diabetes mellitus, particularly poorly controlled, causes hyperglycaemia, activating the polyol pathway whereby sorbitol accumulates in tissues such as the lens, retina and kidneys. Such accumulation of sorbitol increases osmotic and oxidative stress, which leads to many diabetic complications, including cataracts, retinopathy, and nephropathy. Based on these outcomes, AR focuses on the prevention of sorbitol production seems to be a practical therapeutic approach [1].

In our study, the isolated flavonoids indicated an ARI with compound **1** and compound **2** having undegraded IC_{50} of 0.97 ± 0.53 μM and 0.92 ± 0.48 μM, respectively. These values were comparable to the standard inhibitor, d-Saccharic acid 1,4-lactone (IC_{50}: 0.88 ± 0.34 μM). Such findings can be considered relevant since they compared the efficiency of synthetic inhibitors and natural compounds, as the latter can be similar or even more effective than the former, which have toxic side effects and low bioavailability [2].

Further, the *in silico* molecular docking study has been carried out in several recent studies [16,17,18] that gave additional information on the

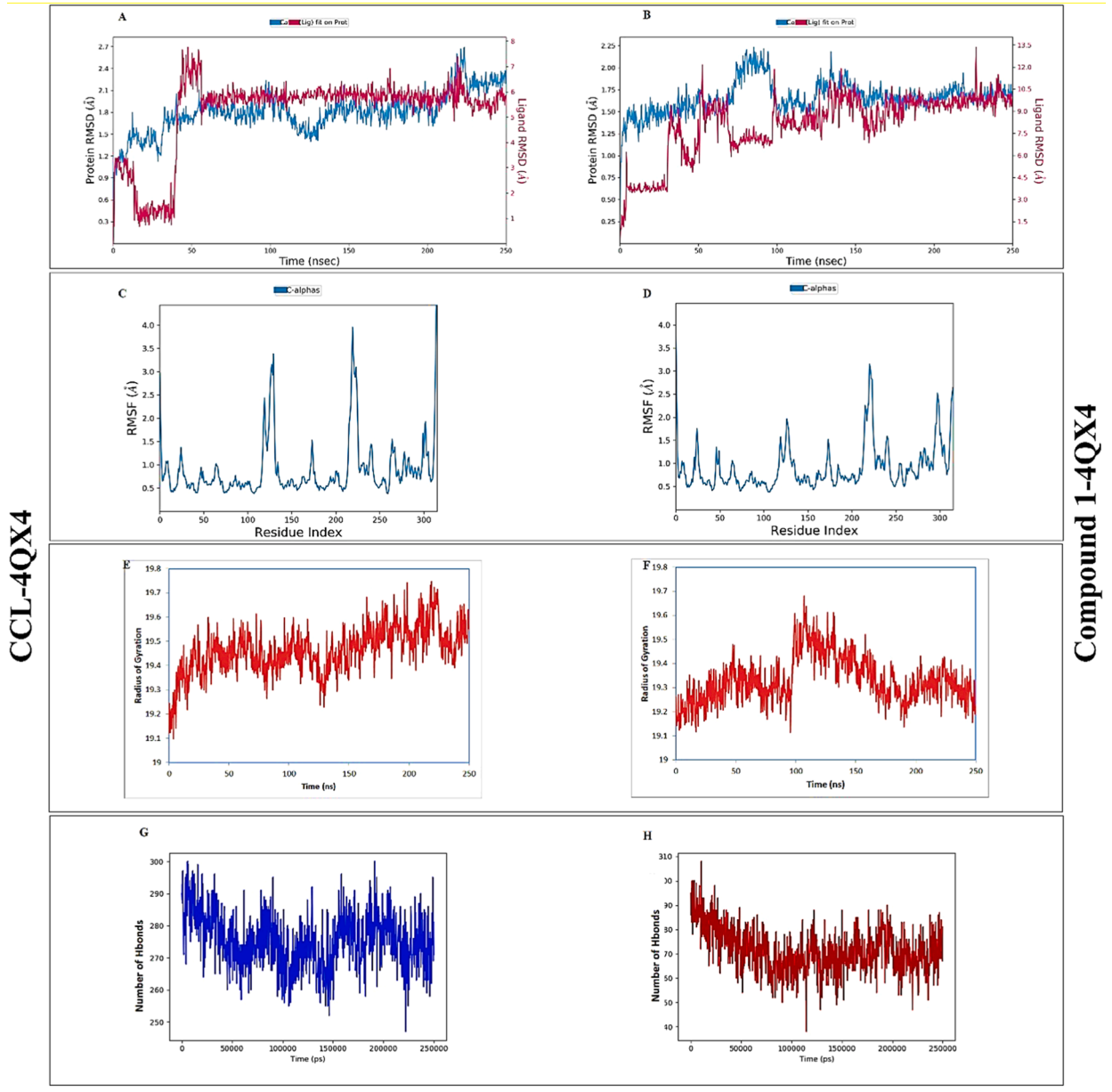

Fig. 7. The graphical variation in root mean square deviation (RMSD), root mean square fluctuation (RMSF), radius of gyration (ROG), and number of hydrogen bond between CCL and isolated compound 1 from E. pulcherrima observed during 250 ns simulation trajectory.

molecular orientation of these flavonoids to AR.The molecular docking studies performed against ALR1 (PDB ID: 4QX4) showed the highest docking score of compound**2** (−10.248 kcal/mol) followed by compound **1** (−9.629 kcal/mol), suggesting strong binding affinity of both compounds against the receptor. Further, the interaction analysis played a crucial role in the stability of the docked complex, highlighting the significance of polar H-bonds and non-polar hydrophobic interactions. These interactions indicated that such flavonoids may inhibit this enzyme at the molecular level, thus eradicating the enzyme's capacity to catalyze glucose to sorbitol transformation. It coheres with the in vitro enzyme inhibition findings and explains the mechanisms responsible for the effects observed from them [3].Additionally, the following residues, Trp20, Tyr48, HOH819, and His110, could be considered hotspot residues of the binding pocket of ALR1 as these residues were involved in maximum interactions with the flavonoids. It was also noteworthy that the observed binding interaction pattern within the predefined active site residues of target protein showed the specificity of compound 1 and 2 within biologically validated allosteric site. Several residues (Trp219, Leu301, Ala299, and Cys298) took part efficiently in stabilizing the compounds. This approach also emphasizes on local receptor ababtabilitythorugh side chain accommodation, thereby mimicking the receptor flexibility. This docking analysis was further supported by MD simulations, revealing the structural stability of the complexes.The results of the current *in silico* analysis also aligned with one such study that investigated the aldose reductase inhibitory potential of natural compounds[36]. Yet another computational study employed a similar analysis to investigate the inhibitory potential of flavonoids against aldose reductase, highlighting the therapeutic potential of flavonoids against AR in managing diabetes mellitus [37].

However, lack of enzyme kinetic studies was not conducted in the present investigation as it had been established through in vitro assays and supported through docking analysis. Consequently, the exact mechanism of inhibition, that is, whether competitive, non-competitive, uncompetitive, remain to be clarified. The kinetic experiments including Lineweaver–Burk and Michaelis–Menten plots will be used in the future work to find out how these flavonoids interact with the enzyme on the

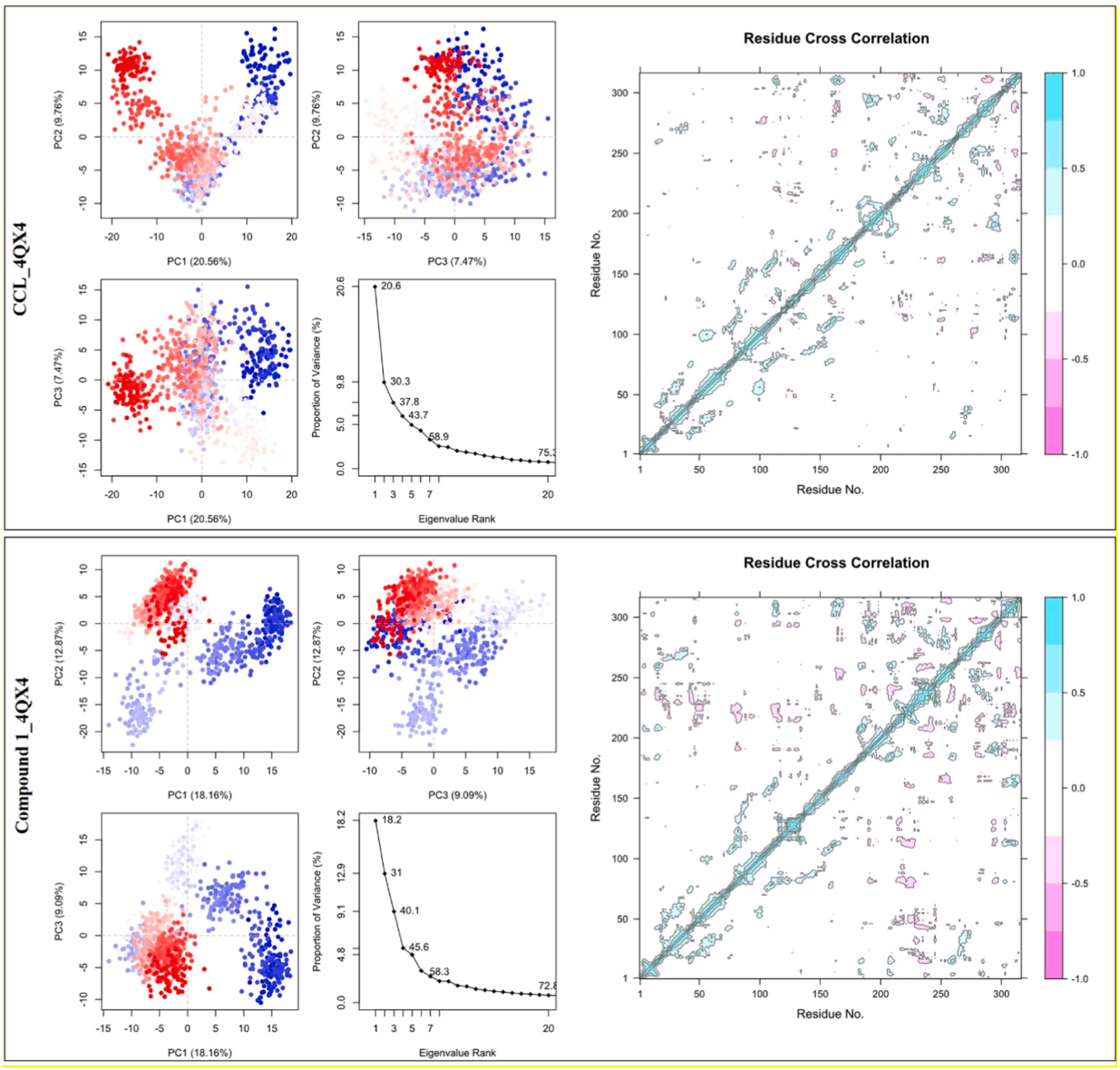

Fig. 8. The graphical variation in Principal component analysis (PCA) and dynamic cross-correlation matrix (DCCM) analysis between CCL and isolated compound 1 from E. pulcherrima observed during 250 ns simulation.

Table 6
Comparative analysis of binding free energies of compound 1, an isolate of E. pulcherrima, with CCL (3E2), calculated through MM-GBSA through a 250-ns simulation trajectory.

Energies (Kcal/mol)	CCL-complex	Compound 1 complex
dG_{bind}	−30.813	−38.458
dG_{bind}Lipo	−9.158	−24.694
dG_{bind}vdW	−27.255	−23.126
dG_{bind} Coulomb	−101.273	−20.150
dG_{bind} H-bond	−4.483	−2.561
dG_{bind} Packing	−0.027	−0.182

mechanistic level. Also, site-directed mutagenesis or time-dependent inhibitor experiments may swing in to prove whether or not the binding takes place at the catalytic or allosteric sites.

The decision for choosing ALR1 as docking and in vitro target was made due to its availability in a pure form along with the availability of a high-resolution X-ray structure (PDB ID: 4QX4). ALR1 has high structural similarity to the human isoform, so it can be used for a preliminary study. None the less, because ALR2 is more directly linked to diabetes complications like neuropathy and retinopathy, subsequent evaluations will incorporate both isoforms to assess selectivity and efficacy.

The investigation of potential inhibitors for their therapeutic use also requires their ADMET analysis for efficient drug design and development. Due to their natural origin, the bioactive application of *E. pulcherrima* flavonoids for treatment and use in safety levers is particularly desirable, more so than synthetic AR inhibitors that are frequently associated with side effects and toxicity. The ADME results were evaluated on the basis of Lipinski's rule of five, which suggested that compound 1 was more likely to be a promising drug-like candidate [38]. Simultaneously, the balanced lipophilicity and solubility of compound 1 make it suitable for interacting in both hydrophilic and hydrophobic environments. Furthermore, the suitable oral bioavailability and feasibility of its synthesis also underscores its significance for drug-like compounds. It should also be taken into account that compound 1 was also highly permeable to the GI membrane with no possible involvement in drug-drug interactions, further pointing towards its therapeutic efficacy. One of the important aspects in drug design and

development is toxicity prediction, which revealed no acute toxicity against both compounds. Moreover, flavonoids are known to have structural features such as hydroxyl groups and conjugated double bonds, making them potential AR inhibitors and increasing their therapeutic effectiveness [8]. Thereby, fragment contribution was also predicted, suggesting the functional groups that could be modified for better structural activity with reduced toxicity and enhanced pharmacological activity. Moreover, the ADMET of flavonoids was also evaluated in several studies, one such study revealed suitable pharmacological and tox profiles of flavonoids, especially compound, revealing its therapeutic potential [39].

Moreover, the chemical reactivity of these flavonoids was also evaluated through DFT studies by applying a similar approach used in recent studies [38]. The overall trend in DFT results showed that higher reactivity of compound 1 due to a smaller energy gap and more softness suggested its likelihood for strong interactions with ALR1. Additionally, the moderate and balanced electrophilicity of compound 1 also made it a promising candidate for favorable interactions with target receptors. Furthermore, the suitable ionization potential and electron affinity of compound 1 also pointed towards its electrophilic and nucleophilic characteristics, which are necessary for biological activities. The MESP surface mapping signifies that compound 1was a promising drug candidate due to its higher reactivity and well-distributed charges over the surface for suitable electrophilic and nucleophilic reactions. These results could also be correlated with another *in silico* study that investigated the potential of phytochemicals by advanced computational strategies, resulting in promising results for natural compounds, specifically for 5,7,8,3′,4′-pentahydroxy-3- methoxyflavone(1) [40]. These studies highlighted the therapeutic potential of compound 1for managing diabetes mellitus type 2.

To gain detailed knowledge of the dynamic behavior of protein bound to compound 1, a 250 ns simulation was run, revealing significant findings on RMSD, RMSF, ROG, and H-bond, while calculating binding free energies through MMGBSA analysis. The results showed that compound 1 maintained equilibrium during the trajectory and exhibited a lower RMSD value (<2.5Å) than the CCL, highlighting the increased structural stability of the target protein upon ligand binding. The RMSF analysis of compound 1 demonstrated slightly decreased flexibility near the loop regions of the alpha chain of the target protein compared to the CCL complex, enhancing the overall stability of the docked complex during the 250 ns simulations. Moreover, ROG indicated protein structural integrity, aligning with the observation that a stable ROG value signifies a well-folded protein structure. The H-bond analysis showed consistent formation of H-bonds but slightly fewer than the CCL, suggesting that the quality and stability of H-bonds are more critical than their quantity in determining the binding affinity of the compounds within the binding site of the target protein. The flexible and stable conformation of ALR1 (PDB ID: 4QX4) was also observed in other studies [41]. Furthermore, the MMGBSA calculations revealed higher binding free energy for compound 1 (−38.458 kcal/mol), highlighting the potential inhibitory efficacy of the compound, which is crucial for drug design. Additionally, increased lipophilicity contributed to desolvation and accurate positioning of compound 1 within the hydrophobic pocket of the target protein. Notably, the CCL complex exhibited higher electrostatic interaction than the compound 1 complex, leading to reduced specificity and increasing the risk of potential off-targets for CCL. These analyses suggested a higher binding affinity for compound 1, underscoring the significance of hydrophobic interactions and optimal ligand pose in achieving a strong and specific interaction with the active residues of the binding pocket, which are crucial for drug design and optimization [42].

Therefore, the findings of this study form the basis for subsequent research on the invention of natural AR inhibitors for diabetes type 2 patient management. Possible directions for the following research are in vivo assessment of chronic safety and effectiveness of these flavonoids and the interaction of these substances with other anti-diabetic medications. Furthermore, there is a need for further studies on the bioavailability and pharmacokinetic properties of compound 1 and compound **2**.

Therefore, flavonoids from *E. pulcherrima* can potentially be a practical class of natural products in treating complications caused by diabetes. Because of the high level of their AR inhibitory activity combined with relative naturalness, they can be considered promising for further clinical trials. This research, therefore, adds to the knowledge base on the possible uses of plant-derived compounds to treat chronic diseases, including diabetes, emphasizing the reduction of acute hyperglycemia-related complications [43].

5. Conclusion

This work shows that the Flavonoids extracted from *E. pulcherrima*, namely compound 1, and compound **2**, exhibited high inhibitory activity against aldose reductase (AR). Compared to the crude extract, the isolated compounds exhibited potent inhibitory activity with approximately 2.5-fold higher IC_{50} value and very close to the standard inhibitor d-Saccharic acid 1,4-lactone value. Thus, the present results show the possibility of using natural plant-derived compounds to control hyperglycemia-related complications in diabetes through inhibiting enzymes involved in the polyol pathway.The findings offer the following significant contributions to understanding *E. pulcherrima* as a natural source of bioactive flavonoids that counteract adverse consequences of chronic hyperglycemia. Through successful competitive inhibition of aldose reductase, these flavonoids could ameliorate or avert further diabetic complications, particularly cataracts, neuropathy, retinopathy, and nephropathy. More importantly, since they are derived from natural sources and are potentially more potent as aldose reductase inhibitors, they can be further explored as safer substitutes for synthetic aldose reductase inhibitors with poor efficacy profiles and often implicated in side effects.

Furthermore, molecular docking analysis also supported the binding of these flavonoids to the active site of aldose reductase, which explained the level of inhibition noted above. This synergy between computational modeling and biochemical experiments deepens the knowledge of such compounds and their application in diabetes treatment.Additionally, *in silico* evaluation of ADME/Tox also underscores the therapeutic potential of these flavonoids, highlighting compound 1 as a promising drug-like candidate with suitable chemical reactivity and balanced charge distribution for electrophilic and nucleophilic attacks. Moreover, the simulations carried out under 250 ns showed structural stability with significant binding and compact nature of compound 1 bound with the target protein in real-time setting. Furthermore, the MMGBSA calculations also revealed strong inhibitory potential of compound 1 (−38.458 kcal/mol) due to higher binding free energy. However, in vivo assays should be investigated for future work. Furthermore, specific structural modification could be applied to increase the activity and selectivity of these flavonoids for aldose reductase. These studies would create a basis for the clinical use of these plants and the fabrication of plant-derived treatments for managing diabetes-related complications.The findings of this study offer an advance toward the discovery of more natural, efficient and safer interventions for preventing/disabling the increasing mundialization of diabetes. Thus, this work provides a basis for innovative solutions to enhance the quality of life for millions of people with diabetes worldwide by using *E. pulcherrima's* therapeutic attributes.

CRediT authorship contribution statement

Rahaf Ajaj: Supervision, Formal analysis, Conceptualization. **Abdur Rauf:** Supervision, Formal analysis, Conceptualization. **Zuneera Akram:** Writing – review & editing, Writing – original draft, Methodology, Investigation, Formal analysis. **Muhammad Umer Khan:** . **Raima Rehman:** Methodology, Investigation. **Zubair Ahmad:** Writing

– review & editing, Writing – original draft, Supervision, Methodology, Formal analysis, Conceptualization. **Yasir Anwar:** Writing – review & editing, Writing – original draft, Formal analysis. **Marcello Iriti:** Writing – review & editing, Writing – original draft, Supervision, Formal analysis, Conceptualization.

Declaration of competing interest

The authors declare that they have no known competing financial interests or personal relationships that could have appeared to influence the work reported in this paper.

Acknowledgment

This Project was funded by the Deanship of Scientific Research (DSR) at King Abdulaziz University, Jeddah, under grant no. (GPIP: 1689–130–2024). The authors, therefore, acknowledge with thanks DSR for technical and financial support.

Supplementary materials

Supplementary material associated with this article can be found, in the online version, at doi:10.1016/j.molstruc.2025.142963.

Data availability

Data will be made available on request.

References

[1] B.A. Memon, K.B. Khalid Bhatti, Diabetes mellit.: chronic metab. disord. (2002).
[2] S. Ahmad, M.F.A. Ahmad, S. Khan, S. Alouffi, M. Khan, C. Prakash, M.W.A. Khan, I. A. Ansari, Exploring aldose reductase inhibitors as promising therapeutic targets for diabetes-linked disabilities, Int. J. Biol. Macromol (2024) 135761.
[3] J.K. Gupta, The role of aldose reductase in polyol pathway: an emerging pharmacological target in diabetic complications and associated morbidities, Curr Pharm Biotechnol 25 (2024) 1073–1081.
[4] M. Singh, A. Kapoor, A. Bhatnagar, Physiological and pathological roles of aldose reductase, Metabolites 11 (2021) 655.
[5] S. Mishra, P. Tiwari, R. Yadav, P.S. Patel, An extensive analysis of diseases associated with diabetes, J. Pharma Insights Res. 2 (2024) 174–187.
[6] T. Hussain, B. Tan, G. Murtaza, G. Liu, N. Rahu, M.S. Kalhoro, D.H. Kalhoro, T. O. Adebowale, M.U. Mazhar, Z. ur Rehman, Flavonoids and type 2 diabetes: evidence of efficacy in clinical and animal studies and delivery strategies to enhance their therapeutic efficacy, Pharmacol. Res 152 (2020) 104629.
[7] R.F. Khan, R.P. Yadav, A. Singh, Screening of pharmacological and biological properties of a euphorbious plant, euphorbia pulcherima: a review, Int. J. Pharmacogn. Pharm. Sci. 3 (2021) 12–15.
[8] A. Basnett, S. Pradhan, R. Das, C. Sharma, To investigate phytochemical parameter, pharmacognostical evaluation, pharmacological (anti-bacterial) activity of the extract of Euphorbia pulcherrima, J. Drug Deliv. Ther. 13 (2023) 60–67.
[9] A.S. Aljohani, F.A. Alhumaydhi, A. Rauf, E.M. Hamad, U. Rashid, In Vivo anti-inflammatory, analgesic, sedative, muscle relaxant activities and molecular docking analysis of phytochemicals from Euphorbia pulcherrima, Evid.-Based Complement. Altern. Med. 2022 (2022) 7495867.
[10] S. Bouknana, M. Bouhrim, H. Ouassou, M. Bnouham, Review of medicinal plants and their compounds for aldose reductase inhibitory activity, Lett Drug Discov 15 (2018) 796–812.
[11] X. Luo, J. Wu, S. Jing, L.-J. Yan, Hyperglycemic stress and carbon stress in diabetic glucotoxicity, Aging Dis 7 (2016) 90.
[12] L.G. Ferreira, R.N. Dos Santos, G. Oliva, A.D. Andricopulo, Molecular docking and structure-based drug design strategies, Molecules 20 (2015) 13384–13421.
[13] A. Rauf, M. Raza, M. Humayun Khan, H.A. Hemeg, Y.S. Al-Awthan, O. Bahattab, S. Bawazeer, S. Naz, F. Basoglu, M. Saleem, In vitro and in silico studies on clinically important enzymes inhibitory activities of flavonoids isolated from Euphorbia pulcherrima, Ann, Med 54 (2022) 495–506.
[14] L.A.-G. Refahy, Study on flavonoids and triterpenoids content of some Euphorbiaceae plants, J. Life Sci. 5 (2011) 100–107.
[15] S. Ahn, Y. Jung, S.Y. Shin, Y.H. Lee, Identification of the active components inhibiting the expression of matrix metallopeptidase-9 by TNFα in ethyl acetate extract of Euphorbia humifusa Willd, J Appl Biol Chem 62 (2019) 367–374.
[16] A. Imran, M.T. Shehzad, S.J.A. Shah, T. Al Adhami, M. Laws, K.M. Rahman, R. D. Alharthy, I.A. Khan, Z. Shafiq, J. Iqbal, Development and exploration of novel substituted thiosemicarbazones as inhibitors of aldose reductase via in vitro analysis and computational study, Sci Rep 12 (2022) 5734.
[17] L.H. Mervin, A.M. Afzal, L. Brive, O. Engkvist, A. Bender, Extending in silico protein target prediction models to include functional effects, Front Pharmacol 9 (2018) 613.
[18] L.H. Mervin, A.M. Afzal, G. Drakakis, R. Lewis, O. Engkvist, A. Bender, Target prediction utilising negative bioactivity data covering large chemical space, J Cheminform 7 (2015) 1–16.
[19] N. Schneider, R.A. Sayle, G.A. Landrum, Get your atoms in order an open-source implementation of a novel and robust molecular canonicalization algorithm, J Chem Inf Model 55 (2015) 2111–2120.
[20] S.S. Antunes, V.W.-H. Rabelo, N.C. Romeiro, Natural products from Brazilian biodiversity identified as potential inhibitors of PknA and PknB of M. tuberculosis using molecular modeling tools, Comput, Biol, Med 136 (2021) 104694.
[21] M. Stefek, M. Soltesova Prnova, M. Majekova, C. Rechlin, A. Heine, G. Klebe, Identification of novel aldose reductase inhibitors based on carboxymethylated mercaptotriazinoindole scaffold, J. Med, Chem 58 (2015) 2649–2657.
[22] A. Mishra, V. Mulpuru, N. Mishra, An interaction network driven approach for identifying cervical, endometrial, vulvar carcinomic biomarkers and their multi-targeted inhibitory agents from few widely available medicinal plants, Appl, Biochem, Biotechnol 195 (2023) 6893–6912.
[23] E. Harder, W. Damm, J. Maple, C. Wu, M. Reboul, J.Y. Xiang, L. Wang, D. Lupyan, M.K. Dahlgren, J.L. Knight, OPLS3: a force field providing broad coverage of drug-like small molecules and proteins, J Chem Theory Comput 12 (2016) 281–296.
[24] D. Seeliger, B.L. de Groot, Conformational transitions upon ligand binding: holo structure prediction from apo conformations, Biophys, J 98 (2010) 428a.
[25] S. Akbar, S. Das, A. Iqubal, B. Ahmed, Synthesis, biological evaluation and molecular dynamics studies of oxadiazine derivatives as potential anti-hepatotoxic agents, J. Biomol. Struct. Dyn. 40 (2022) 9974–9991.
[26] A. Daina, O. Michielin, V. Zoete, SwissADME: a free web tool to evaluate pharmacokinetics, drug-likeness and medicinal chemistry friendliness of small molecules, Sci Rep 7 (2017) 42717.
[27] J.V. Borba, V.M. Alves, R.C. Braga, D.R. Korn, K. Overdahl, A.C. Silva, S.U. Hall, E. Overdahl, N. Kleinstreuer, J. Strickland, STopTox: an in silico alternative to animal testing for acute systemic and topical toxicity, in: Env., Health Perspect, 130, 2022 027012.
[28] M.M. Matin, A.R. Nath, O. Saad, M.M. Bhuiyan, F.A. Kadir, S.B. Abd Hamid, A. A. Alhadi, M.E. Ali, W.A. Yehye, Synthesis, PASS-predication and in vitro antimicrobial activity of benzyl 4-O-benzoyl-α-L-rhamnopyranoside derivatives, Int J Mol Sci 17 (2016) 1412.
[29] E.D. Raczyńska, J.-F. Gal, P.-C. Maria, G.S. Sakhawat, M.Q. Fahim, H. Saeidian, Nitriles with high gas-phase basicity—Part II transmission of the push–pull effect through methylenecyclopropene and cyclopropenimine scaffolds intercalated between different electron donor (s) and the cyano N-protonation site, Molecules 27 (2022) 4370.
[30] T. Tsuneda, J.-W. Song, S. Suzuki, K. Hirao, On Koopmans' theorem in density functional theory, J Chem Phys (2010) 133.
[31] P.W. Hildebrand, A.S. Rose, J.K. Tiemann, Bringing molecular dynamics simulation data into view, Trends Biochem, Sci 44 (2019) 902–913.
[32] M.A. Rasheed, M.N. Iqbal, S. Saddick, I. Ali, F.S. Khan, S. Kanwal, D. Ahmed, M. Ibrahim, U. Afzal, M. Awais, Identification of lead compounds against Scm (fms10) in Enterococcus faecium using computer aided drug designing, Life 11 (2021) 77.
[33] D. Shivakumar, J. Williams, Y. Wu, W. Damm, J. Shelley, W. Sherman, Prediction of absolute solvation free energies using molecular dynamics free energy perturbation and the OPLS force field, J Chem Theory Comput 6 (2010) 1509–1519.
[34] B.J. Grant, L. Skjaerven, X.Q. Yao, The Bio3D packages for structural bioinformatics, Protein Sci. 30 (2021) 20–30.
[35] J. Palma, G. Pierdominici-Sottile, On the uses of PCA to characterise molecular dynamics simulations of biological macromolecules: basics and tips for an effective use, ChemPhysChem 24 (2023) e202200491.
[36] A. Rauf, S. Naz, M.U. Khan, T. Zahid, Z. Ahmad, Z. Akram, M. Khan, Z.A. Shah, W. F. Alsanie, A.S. Alamri, Aldose reductase inhibitory evaluation and in silico studies of bioactive secondary metabolites isolated from Fernandoa. Adenophylla (Wall. ex G. Don), J Mol Struct 1328 (2025) 141308.
[37] M. Yasir, J. Park, E.-T. Han, J.-H. Han, W.S. Park, W. Chun, Investigating the inhibitory potential of flavonoids against aldose reductase: insights from molecular docking, dynamics simulations, and gmx_mmpbsa analysis, Curr Issues Mol Biol 46 (2024) 11503–11518.
[38] M.B. Afridi, H. Sardar, G. Serdaroğlu, S.W.A. Shah, K.F. Alsharif, H. Khan, SwissADME studies and Density Functional Theory (DFT) approaches of methyl substituted curcumin derivatives, Comput Biol Chem 112 (2024) 108153.
[39] S. Jose, S.S. Devi, P. S, K. Al-Khafaji, Phytochemical constituents of Inula britannica as potential inhibitors of dihydrofolate reductase: a strategic approach against shigellosis, J. Biomol. Struct. Dyn. 40 (2022) 11932–11947.
[40] J. Khan, S.A. Sakib, S. Mahmud, Z. Khan, M.N. Islam, M.A. Sakib, T.B. Emran, J. Simal-Gandara, Identification of potential phytochemicals from Citrus limon against main protease of SARS-CoV-2: molecular docking, molecular dynamic simulations and quantum computations, J. Biomol. Struct. Dyn. 40 (2022) 10741–10752.
[41] L.M. Kelam, M.S. Gill, M.E. Sobhia, Revolutionizing diabetes treatment: computational insights into 4-hydroxy isoleucine derivatives and advanced

molecular screening for antidiabetic compounds, Explor. Drug Sci. 3 (2025) 1008104.
[42] L. Dong, X. Qu, Y. Zhao, B. Wang, Prediction of binding free energy of protein–ligand complexes with a hybrid molecular mechanics/generalized born surface area and machine learning method, ACS omega 6 (2021) 32938–32947.
[43] F. Otieno, R. Kagia, Virtual screening for chemical analogues similar to phytochemicals that inhibit aldose reductase in the development of diabetic microvascular complications, F1000Res 12 (2023) 314.